Towards multistranded molecular wires: Syntheses, structures, and reactivities of tetraplatinum bis(polyynediyl) complexes with Pt-C_x-Pt-$(P(CH_2)_3P)_2$-Pt-C_x-Pt-$(P(CH_2)_3P)_2$ cores (x = 4, 6, 8)†

Gareth R. Owen,[a] Sébastien Gauthier,[b] Nancy Weisbach,[b] Frank Hampel,[a] Nattamai Bhuvanesh[b] and John A. Gladysz*[b]

Received 1st February 2010, Accepted 1st April 2010
First published as an Advance Article on the web 7th May 2010
DOI: 10.1039/c002041a

Reactions of *trans*,*trans*-$(C_6F_5)(p\text{-}tol_3P)_2Pt(C{\equiv}C)_nPt(Pp\text{-}tol_3)_2(C_6F_5)$ (**PtC$_x$Pt**; $x = 2n$) and the 1,3-diphosphine $Ph_2P(CH_2)_3PPh_2$ (2.5 equiv) give the tetraplatinum complexes *trans*, *trans*,*trans*,*trans*-$(C_6F_5)\dot{P}t(C{\equiv}C)_nPt(C_6F_5)(PPh_2(CH_2)_3Ph_2P)_2(C_6F_5)Pt(C{\equiv}C)_nPt(C_6F_5)(PPh_2(CH_2)_3Ph_2\dot{P})_2$ (**[Pt′C$_x$Pt′]$_2$**; x = 4/6/8, 39%/95%/81%). Crystal structures of **[Pt′C$_8$Pt′]$_2$** and two solvates of **[Pt′C$_6$Pt′]$_2$** are determined. These confirm that each diphosphine spans two platinum atoms from different $Pt(C{\equiv}C)_nPt$ linkages, as opposed to (1) the 1,2-diphosphine $Ph_2P(CH_2)_2PPh_2$, which under similar conditions with **PtC$_8$Pt** affords the diplatinum bis(chelate) *cis*,*cis*-$(\dot{P}Ph_2(CH_2)_2Ph_2P)(C_6F_5)\dot{P}t(C{\equiv}C)_4\text{-}\dot{P}t(C_6F_5)(PPh_2(CH_2)_2Ph_2\dot{P})$ (73%) or (2) α,ω-diphosphines with longer methylene chains, which span the platinum termini. The formulation **[Pt′C$_4$Pt′]$_2$** is supported by a reaction with PEt_3 (10 equiv) to give *trans*,*trans*-$(C_6F_5)(Et_3P)_2Pt(C{\equiv}C)_2Pt(PEt_3)_2(C_6F_5)$. In **[Pt′C$_8$Pt′]$_2$** and one solvate of **[Pt′C$_6$Pt′]$_2$**, the chains cross at 77.2°–87.7° angles, with the closest interchain carbon–carbon distances (3.27–3.61 Å) less than the sum of the van-der-Waals radii. In the other solvate of **[Pt′C$_6$Pt′]$_2$**, the chains are essentially parallel, and the separation is much greater (4.96 Å). UV-visible spectra show no special electronic interactions. However, cyclic voltammograms indicate irreversible oxidations, in contrast to the partially reversible oxidations of **PtC$_6$Pt** and **PtC$_8$Pt**. The initially formed radical cations are proposed to undergo rapid chain–chain coupling. The new complexes decompose without melting above 185 °C. With **[Pt′C$_8$Pt′]$_2$**, IR spectra indicate the formation of a new C≡C-rich substance.

Introduction

Numerous complexes have now been prepared in which polyynediyl sp carbon chains bridge two transition metal fragments, $L_yM(C{\equiv}C)_nML_y$.[1,2] Much of this interest has been prompted by the rich redox chemistry of such adducts, the unique and often unusual structural[2] and electronic[3] features associated with each redox state,[4] and the obvious connection to molecular wires.[5]

One emerging theme is the use of $M(C{\equiv}C)_nM$ segments as building blocks for architecturally diverse assemblies, such as extended $L_yM[(C{\equiv}C)_nML_y]_z(C{\equiv}C)_nML_y$ arrays[6,7] or molecular polygons $L_yM[(C{\equiv}C)_nML_y]_z(C{\equiv}C)_n$-.[8,9] The first area has been explored by Hagihara, Sonogashira, and others,[6] as well as our own group,[7] and the last by Youngs, Bruce, and Anderson.[8] However, prior to the efforts detailed herein, there have been no reports of structurally authenticated bis(polyynediyl) systems in which the sp chains bridge the same endgroups. Such assemblies can be viewed as multistranded molecular wires.

Our entry into the chemistry described below derived from a consideration of the possible modes by which tetraaryl α,ω-diphosphines with polymethylene backbones, $Ar_2P(CH_2)_mPAr_2$, might bind to square planar diplatinum polyynediyl complexes and related species. As illustrated in Scheme 1 (top), the addition of diphosphines tethered by eight to eighteen methylene groups to butadiynediyl,[10] hexatriynediyl,[10] octatetraynediyl,[11] and dodecahexaynediyl[11] complexes leads to adducts **A** in which the diphosphines span the platinum termini. When the methylene chains are long enough, they coil around the sp chains in striking double helical motifs (**B**).[10-12]

As illustrated in Scheme 1 (bottom), additions of diphosphine ligands with two methylene groups, $Ar_2P(CH_2)_2PAr_2$, would be expected to lead to the bis(chelates) **C** with *cis* geometries. When the platinum substituent X in **C** is amenable to further substitution, these represent potential building blocks for molecular polygons. Although such chelations have not yet been described in the open literature, good precedent is available with related monoplatinum complexes and 1,2-diphosphines.[13] A confirmatory example is included with this report.

Given the limiting coordination modes in Scheme 1, there was a natural curiosity regarding reactions of α,ω-diphosphines tethered by three to six methylene groups. Although 1,3-diphosphine chelates of platinum are well known, such species are usually derived from dichloride complexes *cis*-$(PAr_2(CH_2)_3Ar_2P)PtCl_2$ as opposed to late-stage substitutions as in Scheme 1.[8b,c] In this study, we establish a third binding motif with diplatinum polyynediyl

[a]*Institut für Organische Chemie and Interdisciplinary Center for Molecular Materials, Friedrich-Alexander-Universität Erlangen-Nürnberg, Henkestraße 42, 91054, Erlangen, Germany*
[b]*Department of Chemistry, Texas A&M University, PO Box 30012, College Station, Texas 77842-3012, USA*

† CCDC reference numbers 258765 and 258766. For crystallographic data in CIF or other electronic format see DOI: 10.1039/c002041a

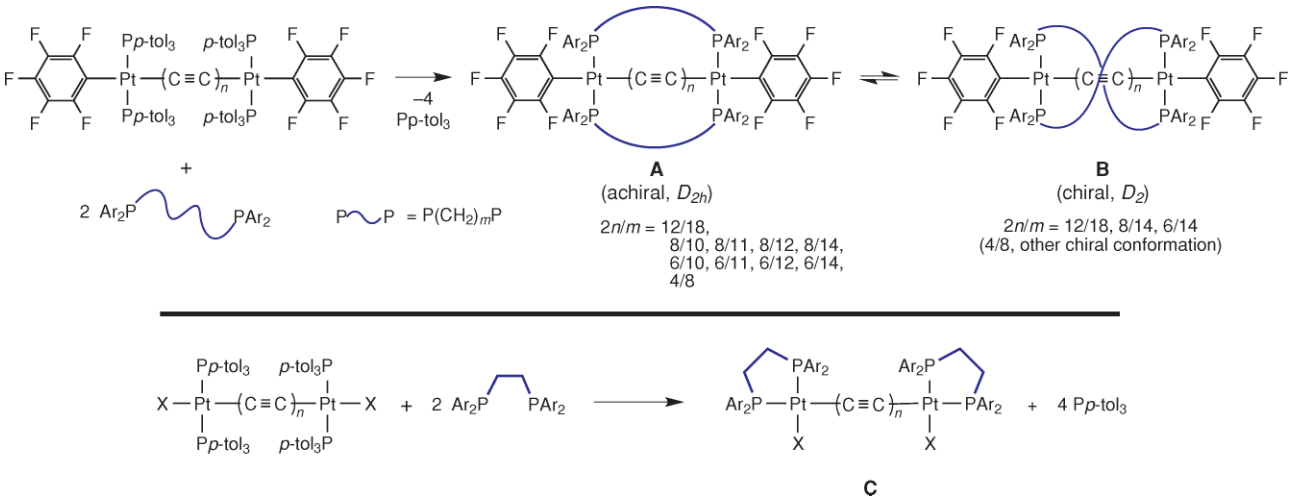

Scheme 1 Limiting reactions of diplatinum polyynediyl complexes with diphosphines $Ar_2P(CH_2)_mPAr_2$: endgroup-spanning products (top) *versus* endgroup-chelating products (bottom).

complexes, namely the assembly of $Pt(C{\equiv}C)_nPt$ segments into "bundles" that are joined by diphosphines at each terminus. The detailed spectroscopic and structural characterization of these adducts, which can adopt confirmations with either parallel or "crossed" sp carbon chains, is described, together with preliminary reactivity data. A portion of this work has been communicated.[14]

Results

1. Syntheses of title compounds

As shown in Scheme 2, a THF solution of the hexatriynediyl complex *trans*,*trans*-$(C_6F_5)(p\text{-}tol_3P)_2Pt(C{\equiv}C)_3Pt(Pp\text{-}tol_3)_2(C_6F_5)$ (**PtC_6Pt**;[10,15] 0.0039 M) was treated with the solid 1,3-diphosphine $Ph_2P(CH_2)_3PPh_2$ (dppp; 2.5 equiv). Subsequent hexane precipitation gave a homogeneous yellow product in 95% yield based upon the structure established below.

A ^1H NMR spectrum (experimental section) showed that the diphosphine had displaced the P*p*-tol_3 ligands. A ^{31}P NMR spectrum exhibited a single signal, indicating that the *trans* geometries at platinum were maintained (δ (ppm, CD_2Cl_2) 13.0 (s, $^1J_{PPt}$ = 2611 Hz[16])). The mass spectrum showed strong ions consistent with the *tetra*platinum complex *trans*,*trans*,*trans*,*trans*-$(C_6F_5)\overline{Pt(C{\equiv}C)_3Pt(C_6F_5)(PPh_2(CH_2)_3Ph_2P)}_2(C_6F_5)\overline{Pt(C{\equiv}C)_3Pt(C_6F_5)(PPh_2(CH_2)_3Ph_2P)}_2$ (**[Pt′C_6Pt′]$_2$**), which also fit the microanalysis. The ^{13}C NMR and IR spectra resembled those of the precursors, suggesting that the sp carbon chains were intact.

Next, an analogous reaction was attempted with the octatetraynediyl complex **PtC_8Pt** (0.0025 M in THF).[10] A yellow powder with an NMR, IR, mass spectrometric, and microanalytical profile (experimental section) appropriate for **[Pt′C_8Pt′]$_2$** was similarly isolated in 81% yield (Scheme 2). The ^{31}P NMR signal was essentially identical to that of **[Pt′C_6Pt′]$_2$** (δ (ppm, CD_2Cl_2) 13.5 (s, $^1J_{PPt}$ = 2606 Hz[16])).

A corresponding reaction with the butadiynediyl complex **PtC_4Pt** (0.00050 M in THF)[10] afforded a white powder that was assigned as **[Pt′C_4Pt′]$_2$**. The mass spectrum showed molecular and other appropriate ions, but the product was only very sparingly soluble in common organic solvents. Such solubilities are typical in cases where the reactions in Scheme 1 (top) yield oligomers or polymers (*e.g.*, $2n/m$ = 8/16).[11] When a hot bromobenzene solution of **[Pt′C_4Pt′]$_2$** was cooled, a mixture of colorless crystals and white powder was obtained. However, the crystals were too small for X-ray analysis. The ^{31}P NMR spectrum was similar to those of the higher homologs (δ (ppm, C_6D_5Br) 14.8 (s, $^1J_{PPt}$ = 2658 Hz[16])).

In previous studies, it has proved possible to displace alkyldiaryl phosphines from diplatinum polyynediyl complexes with PEt_3.[10,11,15] Thus, as shown in Scheme 3, a THF suspension of **[Pt′C_4Pt′]$_2$** and PEt_3 (1 : 10 mol ratio) was stirred at room temperature. After 18 h, a ^{31}P NMR spectrum indicated a 94 : 6 ratio of the previously characterized diplatinum tetrakis(triethyl phosphine) complex *trans*,*trans*-$(C_6F_5)(Et_3P)_2Pt(C{\equiv}C)_3Pt(PEt_3)_2(C_6F_5)$[17] and **[Pt′$C_4$Pt′]$_2$**. No other signals, except for those of $Ph_2P(CH_2)_3PPh_2$ and excess PEt_3, were present. Although this "debundling" supports the formulation **[Pt′C_4Pt′]$_2$**, it should be noted that PEt_3 also similarly reacts with oligomeric species.[11]

Finally, an analogous sequence starting with the dodecahexaynediyl complex **$PtC_{12}Pt$**[10] gave an orange powder, provisionally assigned as **[Pt′C_{12}Pt′]$_2$**, with similar properties ($^{31}P\{^1H\}$ NMR (δ (ppm, THF-d_8) 13.3 (s, $^1J_{PPt}$ = 2565 Hz[16])). However, the material was too insoluble for ^1H and ^{13}C NMR spectra. As observed with **PtC_xPt**[15] and a related series of compounds,[18] the $^1J_{PPt}$ values monotonically decrease as the polyynediyl chains are lengthened (2658 (C_4), 2611 (C_6), 2606 (C_8), 2565 (C_{12}) Hz).

2. Reactions with 1,2- and 1,4-diphosphines

In order to verify the unique coordinating properties of the 1,3-diphosphine $Ph_2P(CH_2)_3PPh_2$, **PtC_8Pt** was similarly treated with the 1,2-diphosphine $Ph_2P(CH_2)_2PPh_2$ (dppe). As shown in Scheme 4, workup gave the expected diplatinum disubstitution product *cis*,*cis*-$\overline{(PPh_2(CH_2)_2Ph_2P)(C_6F_5)Pt(C{\equiv}C)_4Pt(C_6F_5)(PPh_2(CH_2)_2Ph_2P)}$ (**Pt″C_8Pt″**) as a light yellow solid in 73% yield. Although this complex was nearly insoluble in most organic solvents (toluene, $CHCl_3$, CH_2Cl_2, Et_2O, THF, acetone, acetonitrile, DMSO), it was soluble in DMF, and was characterized analogously to the other new complexes (experimental section).

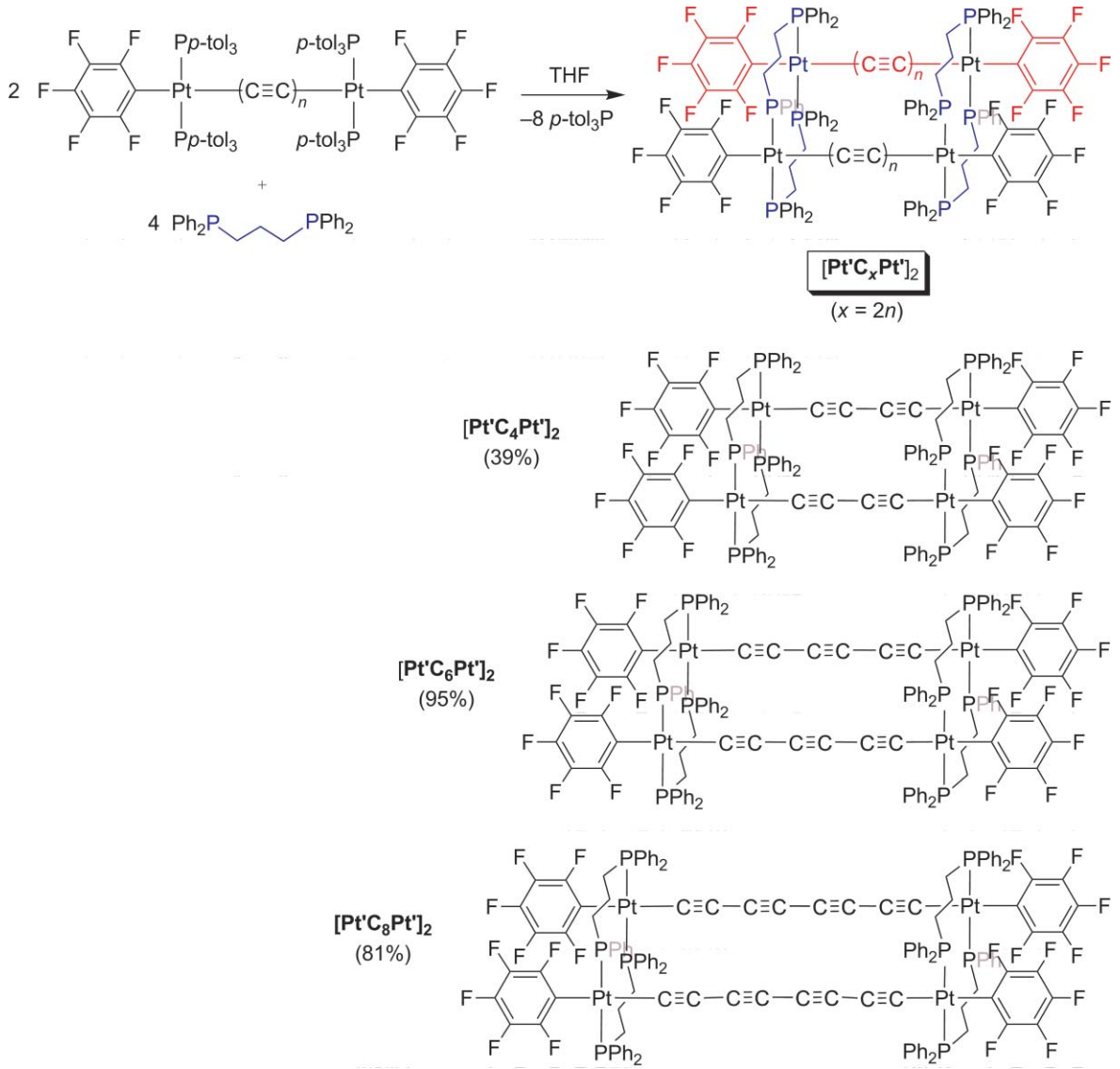

Scheme 2 Syntheses of the title compounds.

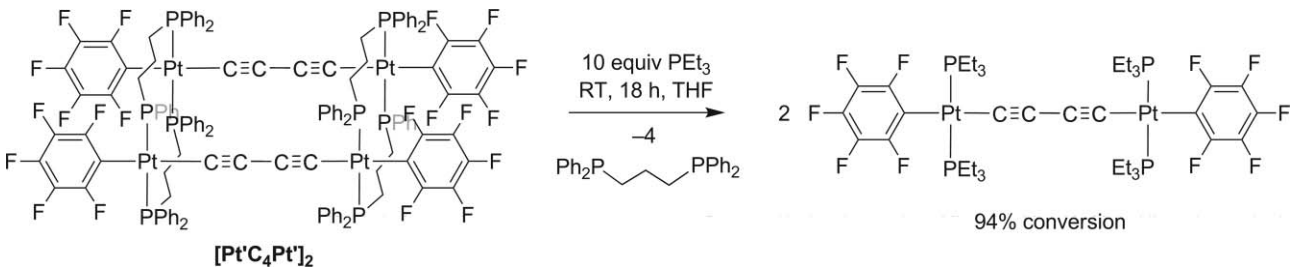

Scheme 3 Debundling of tetraplatinum bis(polyynediyl) complexes with PEt_3.

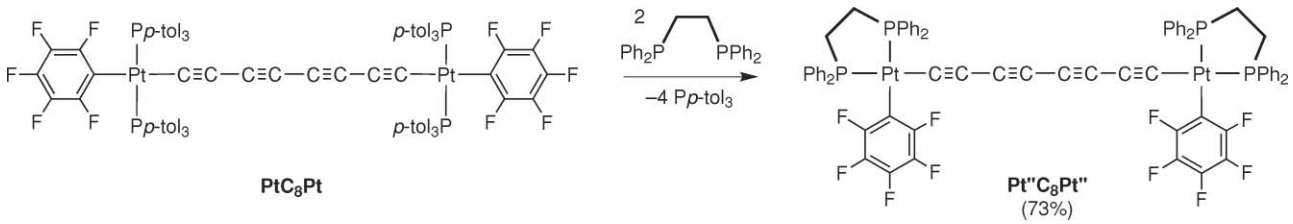

Scheme 4 Reaction of **PtC_8Pt** and a 1,2-diphosphine.

In accord with the *cis* coordination geometry, the ^{31}P NMR spectrum now showed two phosphorus signals, a doublet for the phosphorus atom *trans* to the polyynediyl chain, and a multiplet for that *trans* to the pentafluorophenyl group (δ (ppm, DMF-d_7) 44.74 (d, $^2J_{PP}$ = 6.2 Hz, $^1J_{PPt}$ = 2358 Hz[16]), 41.78–41.59 (m, $^1J_{PPt}$ = 2255 Hz[16])). The $^1J_{PPt}$ values, which are also functions of the coordination geometry,[19] were lower than those of **[Pt′C$_x$Pt′]$_2$** (2358–2255 Hz *vs.* 2658–2565 Hz).

Finally, **PtC$_8$Pt** was analogously treated with the 1,4-diphosphine $Ph_2P(CH_2)_4PPh_2$ (dppb). Subsequent hexane precipitation gave a light yellow solid that was extremely insoluble in common organic solvents. A ^{31}P NMR spectrum could be recorded in THF, and showed only a single signal (δ (ppm) 13.1 (s, $^1J_{PPt}$ = 2551 Hz[16])). The mass spectrum exhibited a strong ion with a mass appropriate for the dppb analog of **[Pt′C$_8$Pt′]$_2$** (positive FAB, *m*/*z* 3345 (M$^+$–H, 100%)). Hence, it was concluded that the binding mode in Scheme 2 can be extended to 1,4-diphosphines.

3. Crystal structures

Crystals of the solvate **[Pt′C$_6$Pt′]$_2$**·4CH_2Cl_2 were grown from CH_2Cl_2–methanol, and the mixed CH_2Cl_2–THF solvate or pseudopolymorph[20] **[Pt′C$_6$Pt′]$_2$**·5CH_2Cl_2·2C_4H_8O was fortuitously isolated from a reaction mixture. Crystals of another mixed solvate, **[Pt′C$_8$Pt′]$_2$**·0.7C_6H_{14}·2C_4H_8O, were obtained from THF–hexane. The X-ray crystal structures were determined as outlined in Table 1 and the experimental section. Key metrical parameters are collected in Table 2.

Three views of each of the three structures are depicted in Fig. 1–3. In the bottom views, the phenyl groups on the phosphorus atoms have been removed and key atoms numbered. The $Ph_2P(CH_2)_3PPh_2$ ligands clearly span two platinum atoms belonging to different Pt(C≡C)$_n$Pt linkages, confirming the above structural assignments. The net result is a "bundle" of two sp carbon chains with twelve-membered-ring termini of the formula $\acute{P}tPPh_2(CH_2)_3Ph_2PPtPPh_2(CH_2)_3Ph_2\acute{P}$.

Both **[Pt′C$_6$Pt′]$_2$**·4CH_2Cl_2 and **[Pt′C$_8$Pt′]$_2$**·0.7C_6H_{14}·2C_4H_8O feature a C_2 symmetry axis. These are best visualized in the bottom representations in Fig. 1 and 3 (*e.g.*, with reference to shapes of the thermal ellipsoids of the fluorine atoms in the latter). That in **[Pt′C$_6$Pt′]$_2$**· 4CH_2Cl_2 is defined by the midpoints of the platinum–platinum vectors on each terminus and passes through the twelve-membered rings. That in **[Pt′C$_8$Pt′]$_2$**·0.7C_6H_{14}·2C_4H_8O is defined by the midpoints of the platinum–platinum vectors involving opposite termini and sp chains. It is oriented vertically, behind the midpoint of the C4–C5 bond. The former C_2 axis exchanges Pt1 with Pt2 and Pt3 with Pt4, whereas the latter exchanges Pt1 with Pt4 and Pt2 with Pt3.

In contrast, **[Pt′C$_6$Pt′]$_2$**·5CH_2Cl_2·2C_4H_8O exhibits an inversion center at the middle of the rectangle defined by the four platinum atoms (three orthogonal S_2 symmetry axes). This exchanges Pt1 with Pt4 and Pt2 with Pt3. In all complexes, there are no symmetry relationships within the Pt1–C$_x$–Pt3 linkages or between the ligands on the Pt1/Pt3 termini. Hence, the attendant bond lengths and angles are contrasted in Table 2. Additional structural features are analyzed in the discussion section.

Table 1 Summary of crystallographic data

Complex	[Pt′C$_6$Pt′]$_2$·4CH_2Cl_2	[Pt′C$_6$Pt′]$_2$·5CH_2Cl_2·2C_4H_8O	[Pt′C$_8$Pt′]$_2$·0.7C_6H_{14}·2C_4H_8O
Empirical Formula	$C_{148}H_{112}Cl_8F_{20}P_8Pt_4$	$C_{157}H_{130}Cl_{10}F_{20}O_2P_8Pt_4$	$C_{160.20}H_{129.80}F_{20}O_2P_8Pt_4$
Formula weight	3582.10	3881.22	3494.96
T/K	173(2)	173(2)	110(2)
Wavelength/Å	0.71073	0.71073	0.71073
Diffractometer	Nonius Kappa CCD	Nonius Kappa CCD	Bruker APEX 2
Crystal system	Orthorhombic	Monoclinic	Orthorombic
Space group	*Pbcn*	$P2_1/c$	*Pccn*
Unit cell dimensions:			
a/Å	26.5408(4)	18.9198(3)	20.797(5)
b/Å	22.3417(5)	22.0175(3)	37.352(11)
c/Å	23.4476(5)	19.5265(2)	20.756(6)
α (°)	90	90	90
β (°)	90	101.2807(8)	90
γ (°)	90	90	90
V/Å^3	13903.6(5)	7976.94(19)	16123(8)
Z	4	2	4
ρ calcd/Mg m^{-3}	1.711	1.587	1.440
μ/mm^{-1}	4.336	3.851	3.610
F(000)	6992	3740	6876
Crystal size/mm	0.25 × 0.25 × 0.02	0.20 × 0.20 × 0.20	0.30 × 0.03 × 0.03
Θ range	1.19 to 27.47	1.41 to 27.48	1.49 to 22.50
Index ranges (*h*,*k*,*l*)	–34,34; –28,28; –30,30	–24,24; –28,28; –25,25	–22,22; –40,40; –22,22
Reflections collected	29643	34584	119008
Independent Reflections	15811 [*R*(int) = 0.0391]	18238 [*R*(int) = 0.0285]	10504 [*R*(int) = 0.1555]
Reflections [$I2\sigma(I)$]	10063	14180	7758
Max. and min. transmission	0.9183 and 0.4103	0.5157 and 0.5157	0.8994 and 0.4106
Data / restraints / parameters	15811 / 6 / 816	18238 / 4 / 906	10504 / 57 / 854
Goodness-of-fit on F^2	1.054	1.097	1.045
Final *R* indices [$I2\sigma(I)$]	R_1 = 0.0431, wR_2 = 0.1030	R_1 = 0.0442, wR_2 = 0.1410	R_1 = 0.0434, wR_2 = 0.1014
R indices (all data)	R_1 = 0.0862, wR_2 = 0.1268	R_1 = 0.0626, wR_2 = 0.1540	R_1 = 0.0711, wR_2 = 0.1124
Largest diff. peak/hole/e Å^{-3}	1.578 and –1.524	4.285 and –1.500	1.195/–0.934

Table 2 Key crystallographic distances (Å) and bond or plane/plane angles (°)

Complex	[Pt′C$_6$Pt′]$_2$·4CH$_2$Cl$_2$[a]	[Pt′C$_6$Pt′]$_2$·5CH$_2$Cl$_2$·2C$_4$H$_8$O[a]	[Pt′C$_8$Pt′]$_2$·0.7C$_6$H$_{14}$·2C$_4$H$_8$O[a]
Pt(1)–C(1)	2.010(6)	2.001(7)	1.973(9)
C(1)≡C(2)	1.203(8)	1.209(9)	1.215(11)
C(2)–C(3)	1.378(9)	1.353(9)	1.347(13)
C(3)≡C(4)	1.210(9)	1.214(10)	1.221(12)
C(4)–C(5)	1.371(9)	1.395(10)	1.361(13)
C(5)≡C(6)	1.225(9)	1.208(9)	1.207(12)
C(6)–C(7)	—	—	1.348(13)
C(7)≡C(8)	—	—	1.211(11)
C(8)–Pt(3) or C(6)–Pt(3)	2.003(6)	1.983(7)	1.986(9)
Pt(1)···Pt(2)	5.642	5.702	5.642
Pt(3)···Pt(4)[a]	5.615	—[b]	—[b]
Pt(1)···Pt(3)	10.3066(4)	10.2616(3)	12.842
Pt(1)···Pt(4)	10.373	11.8633(4)	12.003
Pt(2)···Pt(3)[a]	—[c]	11.6142(5)	12.985
Sum of bond lengths, Pt(1) to Pt(3)	10.400	10.363	12.869
Pt(1)–P(1)	2.2958(17)	2.2975(15)	2.290(2)
Pt(1)–P(2)	2.3014(17)	2.3112(14)	2.300(2)
Pt(3)–P(5)	2.3093(18)	2.3051(14)	2.303(2)
Pt(3)–P(6)	2.3059(18)	2.2902(15)	2.285(2)
Pt(1)–C$_{ipso}$[d]	2.080(6)	2.063(6)	2.062(9)
Pt(3)–C$_{ipso}$[d]	2.065(6)	2.057(6)	2.056(9)
P(1)–Pt(1)–P(2)	173.10(7)	170.66(5)	175.05(8)
P(5)–Pt(3)–P(6)	174.57(6)	174.93(6)	172.74(8)
Pt(1)–C(1)–C(2)	175.8(6)	175.9(6)	176.0(8)
C(1)–C(2)–C(3)	178.1(8)	176.0(8)	176.2(10)
C(2)–C(3)–C(4)	176.1(8)	175.0(8)	178.3(10)
C(3)–C(4)–C(5)	178.1(9)	175.8(8)	179.2(11)
C(4)–C(5)–C(6)	176.0(8)	173.9(8)	177.3(10)
C(5)–C(6)–C(7)	—	—	178.1(10)
C(6)–C(7)–C(8)	—	—	176.6(10)
C(7)–C(8)–Pt(3) or C(5)–C(6)–Pt(3)	170.9(6)	174.8(6)	175.0(7)
C$_{ipso}$–Pt(1)–C(1)[d]	176.8(3)	174.3(2)	177.3(3)
C$_{ipso}$–Pt(3)–C(6) or C$_{ipso}$–Pt(3)–C(8)[d]	175.1(3)	176.7(2)	177.0(4)
C(1)–Pt(1)–P(1)	87.10(18)	85.82(19)	89.4(2)
C(1)–Pt(1)–P(2)	90.41(18)	85.31(19)	85.7(2)
C(6)–Pt(3)–P(5) or C(8)–Pt(3)–P(5)	86.09(19)	89.38(18)	85.2(2)
C(6)–Pt(3)–P(6) or C(8)–Pt(3)–P(6)	88.66(19)	86.09(18)	87.6(2)
C$_{ipso}$–Pt(1)–P(1)[d]	91.11(19)	91.05(16)	93.3(2)
C$_{ipso}$–Pt(1)–P(2)[d]	91.65(18)	98.03(16)	91.6(2)
C$_{ipso}$–Pt(3)–P(5)[d]	90.8(2)	93.42(16)	93.5(3)
C$_{ipso}$–Pt(3)–P(6)[d]	94.4(2)	91.17(16)	93.7(3)
Pt(1)–P(1)–C(12)	111.2(2)	110.8(2)	111.2(3)
Pt(1)–P(2)–C(9)	112.8(2)	111.86(19)	113.1(3)
Pt(3)–P(5)–C(15)	111.1(2)	111.3(2)	113.5(3)
Pt(3)–P(6)–C(18)	110.3(2)	112.1(2)	110.2(3)
C$_{ipso}$–Pt(1)–P(1)–C(12)[d]	111.4(3)	–128.7(3)	123.8(4)
C$_{ipso}$–Pt(1)–P(2)–C(9)[d]	–152.5(3)	139.2(3)	–131.4(4)
C$_{ipso}$–Pt(3)–P(5)–C(18)[d]	–124.3(3)	–122.5(3)	–139.9(4)
C$_{ipso}$–Pt(3)–P(6)–C(15)[d]	123.9(3)	130.8(3)	122.3(4)
Pt(1)–P(1)–C(12)–C(13)	–39.0(5)	42.3(6)	–47.0(7)
Pt(1)–P(2)–C(9)–C(10)	51.6(6)	–56.9(4)	50.4(7)
Pt(3)–P(5)–C(18)–C(19)	40.1(5)	45.1(5)	50.9(7)
Pt(3)–P(6)–C(15)–C(16)	–53.0(5)	–41.4(6)	–48.6(6)
P(1)–C(12)–C(13)–C(14)	–171.5(4)	157.1(5)	168.4(6)
P(2)–C(9)–C(10)–C(11)	–146.8(5)	–171.5(4)	–168.1(6)
P(5)–C(18)–C(19)–C(20)	177.9(4)	172.8(4)	–178.5(6)
P(6)–C(15)–C(16)–C(17)	–155.8(5)	–173.9(5)	173.9(6)
[P(1)–Pt(1)–P(2)]–Pt(3) *vs.* [P(5)–Pt(3)–P(6)]–Pt(1)[e]	85.5	0.8	102.1
[P(1)–Pt(1)–P(2)–C$_{ipso}$] *vs.* [P(5)–Pt(3)–P(6)–C$_{ipso}$][d,e]	78.9	25.0	101.6
[C(1)–P(1)–Pt(1)–P(2)–C$_{ipso}$] *vs.* [C(6)–P(5)–Pt(3)–P(6)–C$_{ipso}$] or [C(8)–P(5)–Pt(3)–P(6)–C$_{ipso}$][d,e]	80.1	20.6	101.8
Pt(1)–Pt(2)–Pt(3) *vs.* Pt(2)–Pt(3)–Pt(4)[e]	87.7	0	77.2
C$_6$F$_5$/C$_6$H$_5$ centroid–centroid distances	4.074	3.849	3.612
	3.702	3.597	3.975
	3.756	4.796	4.036
	3.882	3.769	4.386
average C$_6$F$_5$/C$_6$H$_5$ centroid–centroid distances	3.854	4.003	4.002
intramolecular C$_{sp}$–C$_{sp}$ distance[f]	3.606	4.955	3.271
intermolecular C$_{sp}$–C$_{sp}$distance[f]	10.795	10.972	9.049

[a] As described more fully in the text, the three complexes exhibit different symmetry elements: a C_2 axis exchanging Pt(1) with Pt(2) and Pt(3) with Pt(4), an inversion center exchanging Pt(1) with Pt(4) and Pt(2) with Pt(3), and a C_2 axis exchanging Pt(1) with Pt(4) and Pt(2) with Pt(3), respectively. Thus, certain metrical parameters are degenerate in some complexes but not others. However, in all cases there are no symmetry relationships involving the atoms bound to or between Pt(1) and Pt(3). [b] Identical to Pt(1)···Pt(2). [c] Identical to Pt(1)···Pt(4). [d] C$_{ipso}$ denotes the platinum-bound carbon of C$_6$F$_5$. [e] The values represent the angle between the planes defined by the atoms indicated. [f] The values represent the shortest C$_{sp}$–C$_{sp}$ distance between atoms of nearest chains.

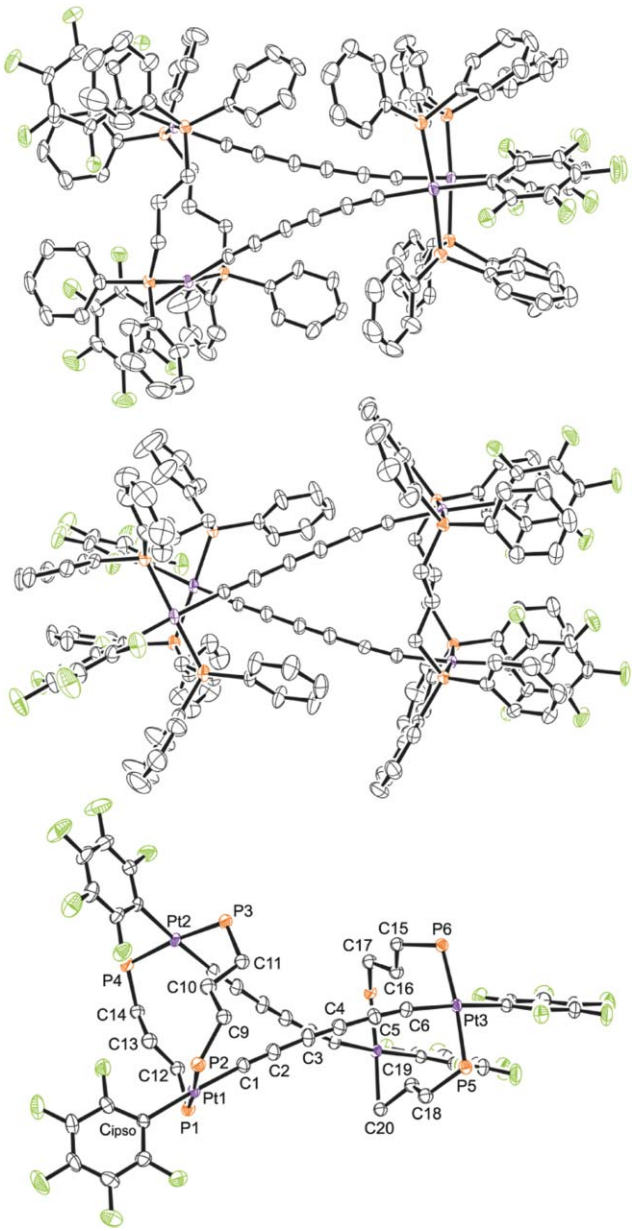

Fig. 1 Thermal ellipsoid plots (50% probability level) of the crystal structure of $[\mathbf{Pt'C_6Pt'}]_2 \cdot 4CH_2Cl_2$. Top and middle: with solvent molecules omitted; bottom: with solvent molecules and phenyl groups omitted.

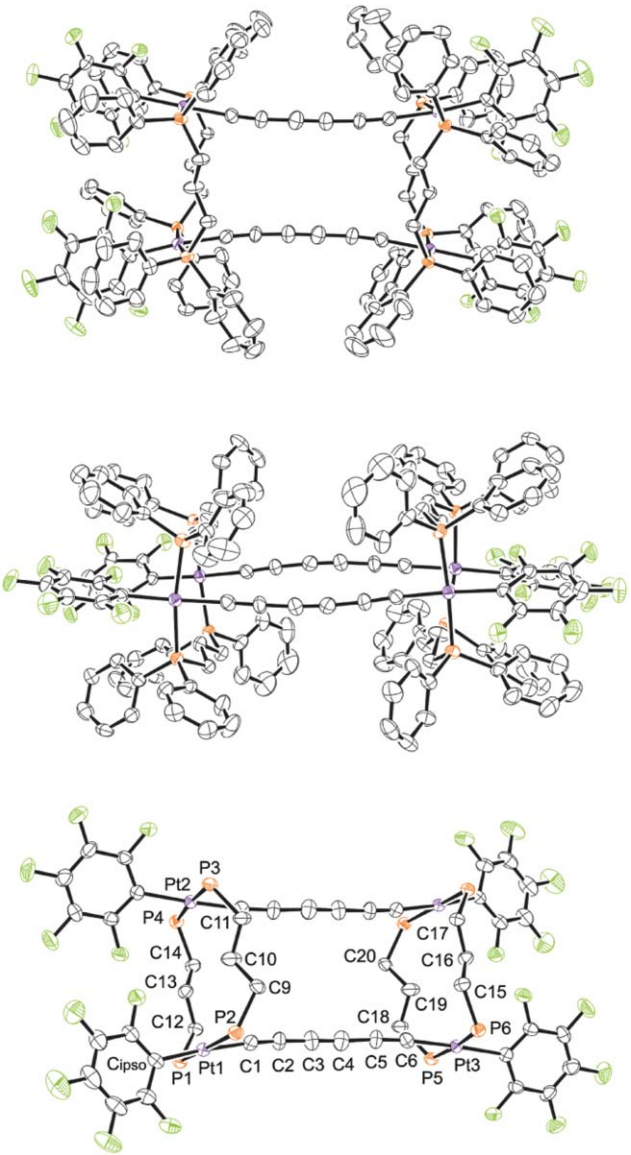

Fig. 2 Thermal ellipsoid plots (50% probability level) of the crystal structure of $[\mathbf{Pt'C_6Pt'}]_2 \cdot 5CH_2Cl_2 \cdot 2C_4H_8O$. Top and middle: with solvent molecules omitted; bottom: with solvent molecules and phenyl groups omitted.

4. Other physical and chemical properties

The NMR properties of $\mathbf{[Pt'C_xPt']_2}$ followed trends previously documented for the diplatinum complexes $\mathbf{PtC_xPt}$.[15] However, since the PPh_2 groups become diastereotopic, two sets of ^{13}C NMR signals were observed. Similarly, the UV-visible spectra of $\mathbf{[Pt'C_6Pt']_2}$ and $\mathbf{[Pt'C_8Pt']_2}$ were quite close to those of their diplatinum counterparts,[15] as summarized in Table 3. In an idealized limit without chain–chain interactions, band broadening, *etc.*, the ε values of the former should be twice the latter, as opposed to the average factor of *ca.* 1.5 observed. In any event, this suggests only minor chain–chain electronic interactions. The nature of the electronic transitions have been analyzed in detail elsewhere.[21]

The thermal behavior of the title complexes was probed. The adducts $\mathbf{[Pt'C_6Pt']_2}$ and $\mathbf{[Pt'C_8Pt']_2}$ decomposed without melting at *ca.* 220 °C and 186 °C, respectively (capillary thermolyses). TGA experiments showed the onset of mass loss at 266–269 °C. With $\mathbf{[Pt'C_4Pt']_2}$, there was no significant decomposition until temperatures of 269–275 °C were reached. Between 200 and 250 °C, the IR $\nu_{C\equiv C}$ bands of $\mathbf{[Pt'C_8Pt']_2}$ at 2150 and 2007 cm^{-1} were replaced by that of a new C≡C-rich substance at 2077 cm^{-1}.

The redox properties of $\mathbf{[Pt'C_6Pt']_2}$ and $\mathbf{[Pt'C_8Pt']_2}$ were probed by cyclic voltammetry. In contrast to the precursors $\mathbf{PtC_6Pt}$ and $\mathbf{PtC_8Pt}$, which undergo partially reversible one electron oxidations to radical cations,[10,15] the tetraplatinum complexes exhibit irreversible behavior characteristic of very rapid consecutive EC processes. A plausible rationale for this difference would involve chain/chain coupling or carbon–carbon bond formation in the initially formed radical cation, as sketched in Scheme 5. We

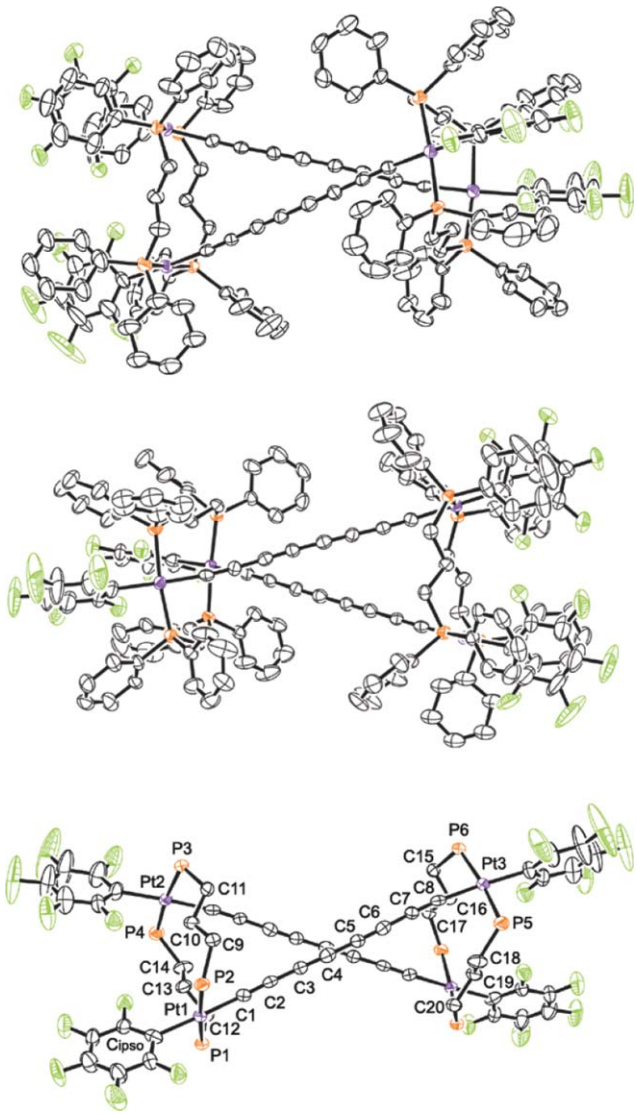

Fig. 3 Thermal ellipsoid plots (50% probability level) of the crystal structure of $[\mathbf{Pt'C_8Pt'}]_2 \cdot 0.7C_6H_{14} \cdot 2C_4H_8O$. Top and middle: with solvent molecules omitted; bottom: with solvent molecules and phenyl groups omitted.

have previously suggested that analogous intermolecular processes contribute to the progressively lower stabilities of bimetallic radical cations $[M(C{\equiv}C)_nM]^{+\bullet}$ as the chains lengthen and become sterically more accessible.[15,22]

To date, well defined chain–chain coupling reactions of $\mathbf{[Pt'C_xPt']_2}$ have remained elusive. In one case, air oxidized samples of $\mathbf{[Pt'C_6Pt']_2}$ afforded small quantities of crystals. Although X-ray analysis did not give a complete structure solution, refinement clearly revealed a species with a R(C=O)–C(R)=C(R)–(C=O)R core, as represented in Scheme 5. Additional support for this assignment was obtained from a mass spectrum, which showed a molecular ion (positive FAB; m/z 3274, M^+), and an IR spectrum, which showed a band consistent with a C=O linkage ($\nu_{C=O}$ 1636 cm^{-1}, br m; $\nu_{C{\equiv}C}$ 2080 cm^{-1}, br m). Analogous oxidation products have been obtained when simple organic monoacetylenes are treated with $Fe(ClO_4)_3$ or PbO_2.[23]

Discussion

1. Syntheses: Strategic considerations and related complexes

The new reactions in Schemes 2 and 4, together with the known reactions in Scheme 1 (top), establish a continuum of reactivity modes for α,ω-diphosphines $Ar_2P(CH_2)_mPAr_2$ and diplatinum polyynediyl complexes $\mathbf{PtC_xPt}$. When the sp^3 methylene chains in the diphosphines are sufficiently long relative to the sp chains, diplatinum complexes in which the diphosphines *span* the platinum termini can be isolated (**A**/**B** in Scheme 1).[10-12] However, when the methylene chains are longer still (*e.g.*, $2n/m = 8/{\geq}16$), the nearly exclusive formation of oligomers and polymers is observed.

Scheme 2, and the analogous reaction of $\mathbf{PtC_8Pt}$ and the 1,4-diphosphine $Ph_2P(CH_2)_4PPh_2$, show that when the methylene chain is too short to span the termini, independent $Pt(C{\equiv}C)_nPt$ assemblies can be tethered, resulting in "bundled" tetraplatinum species. Although oligomerization and polymerization can presumably compete here as well, we believe that the products isolated in Scheme 2 are homogeneous molecular species, despite the skeptical tone in analyzing certain data above. Many types of diplatinum polyynediyl complexes are sparingly soluble or insoluble in common organic solvents, as exemplified by $\mathbf{Pt''C_8Pt''}$ (Scheme 4), significant quantities of which could only be dissolved in DMF.

However, it should be emphasized that insoluble oligomers can be analytically "silent", invisible to spectroscopic and mass spectrometric probes and with the same calculated microanalytical values as the monomers. In this context, diplatinum polyynediyl complexes with P*p*-tol_2-containing ligands are known to be much more soluble than PPh_2 analogs.[17] Thus, in hindsight, the use of alkyl-substituted α,ω-diphosphines such as *p*-$tol_2P(CH_2)_mPp$-tol_2 or $(p\text{-}t\text{-}BuC_6H_4)_2P(CH_2)_mP(p\text{-}C_6H_4\text{-}t\text{-}Bu)_2$[24] might have simplified this study.

Scheme 4 establishes yet another reactivity mode for 1,2-diphosphines $Ar_2P(CH_2)_2PAr_2$, namely the formation of

Table 3 UV-visible and cyclic voltammetry [a]data

Complex	Absorptions/nm [ε/M^{-1} cm^{-1}]	$E_{p,a}$/V	$E_{p,c}$/V	$E°$/V	ΔE/mV	$i_{c/a}$
$\mathbf{PtC_6Pt}$	315 [44000], 345 [15000], 358 [11000], 369 [9000][b]	1.156	1.066	1.111	90	0.71
$\mathbf{[Pt'C_6Pt']_2}$	307 [60000], 342 [25600], 367 [14500][c]	1.193	0.052[d]	0.622	1000	0.16
$\mathbf{PtC_8Pt}$	294 [88000], 326 [126000], 356 [7000], 383 [6000], 414 [3000][b]	1.261	1.143	1.202	118	0.48
$\mathbf{[Pt'C_8Pt']_2}$	310 [129000], 322 [193000], 352 [12600], 379 [9800], 410 [6000][c]	1.284	0.114[d]	0.699	1000	0.06

[a] Conditions: (7–9) × 10^{-3} M n-Bu_4N^+ BF_4^-/CH_2Cl_2 at 22.5 ± 1 °C; Pt working and counter electrodes, potential *vs.* Ag wire pseudoreference; scan rate, 100 mV s^{-1}; ferrocene = 0.46 V. [b] 1.25 × 10^{-6} M in CH_2Cl_2; data from reference 10 or 15. [c] 1.25 × 10^{-5} M in CH_2Cl_2. [d] This peak is poorly defined and is primarily used to set an upper limit for the $i_{c/a}$ value.

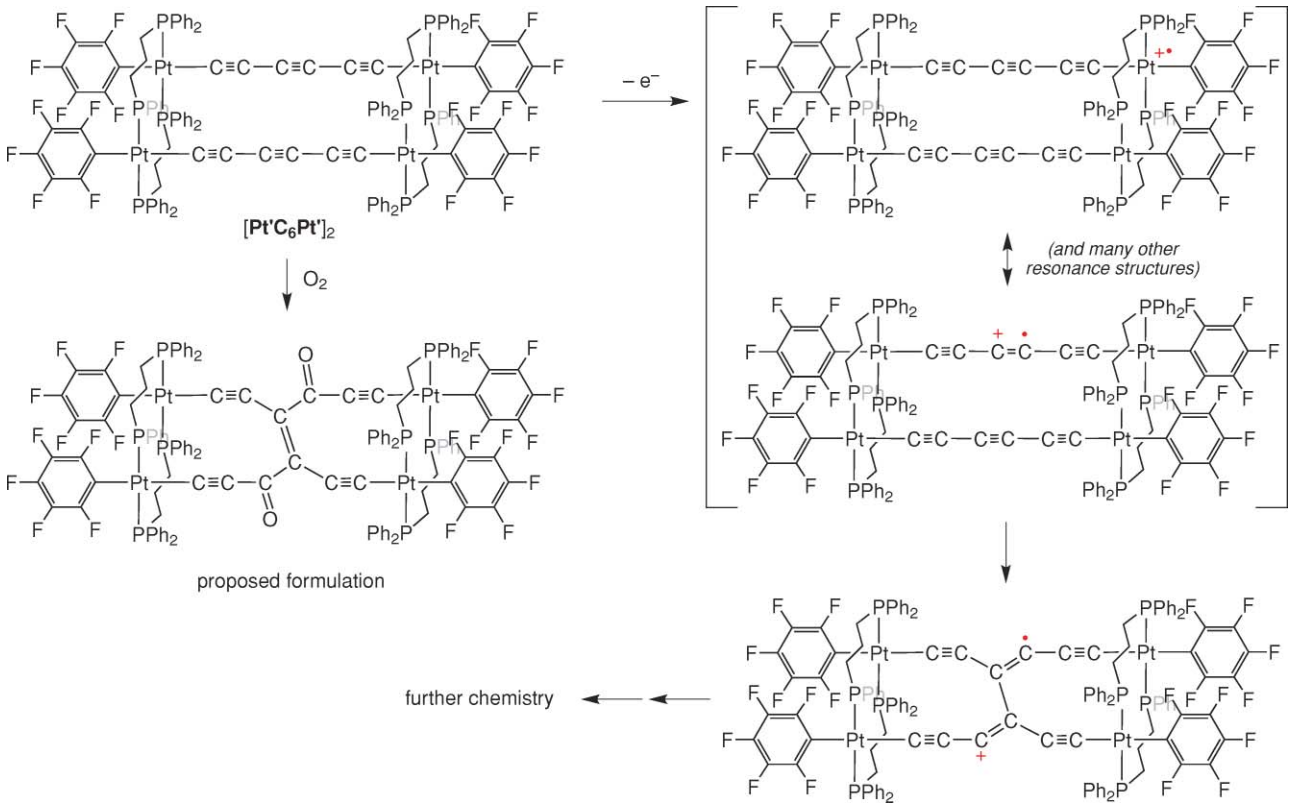

Scheme 5 Possible oxidation reactions.

simple *cis* chelates. In a complementary report by Tykwinski,[13b] two platinum bis(ethynyl) complexes *trans*-$(Ph_3P)_2Pt(C{\equiv}CR)_2$ were treated with a series of five 1,2-diphosphines. In each case, *cis* monoplatinum chelates were isolated in good yields. Interestingly, with the one 1,3-diphosphine assayed, (*S*,*S*)-$Ph_2PCH(CH_3)CH_2CH(CH_3)PPh_2$, good evidence was obtained (R = *p*-tol) for a "bundled" *trans* diplatinum product, with a single twelve membered ring analogous to those on each terminus in **[Pt′C$_x$Pt′]$_2$**. The 1,4-diphosphine DIOP gave a mixture of unidentified products.

The ultimate limit in this series of reactions would involve 1,1-diphoshines, $Ar_2PCH_2PAr_2$. Although these remain to be tested, there is an extensive chemistry of diplatinum polyalkynyl adducts of such ligands, with the *trans*,*trans* system **D** in Fig. 4 representing one large family.[25,26] Such species are normally accessed from the monoplatinum precursor *cis*-$(\overline{PPh_2CH_2Ph_2P})PtCl_2$. These have potential as alternative platforms for the construction of polyplatinum polyynediyl complexes with closely spaced parallel sp carbon chains.

There are many molecules in which two or more $M(C{\equiv}C)_nM$ segments are present. The polygons mentioned in the introduction are notable examples. However, to our knowledge, there has only been one previous report of a system in which two polyynediyl ligands bridge the same endgroup, namely the tetragold bis(butadiynediyl) complex **E** in Fig. 4.[9] This structure is consistent with all IR and NMR data, and mass spectra gave molecular ions or adducts thereof. However, a confirmatory crystal structure is not yet available.

There is also a growing coordination chemistry of polyynediyl based diphosphines, $Ph_2P(C{\equiv}C)_nPPh_2$. For $n = 2$, these have been elaborated into bimetallic complexes of the type **F** in Fig. 4.[27] This represents another way of bringing two sp carbon chains in close proximity, although in contrast to **[Pt′C$_x$Pt′]$_2$** and **E** they are capped with insulating phosphorus atoms. The sp chains are "crossed" in the complexes structurally characterized to date, and some well-defined transannular reactions have been realized.[27b,c]

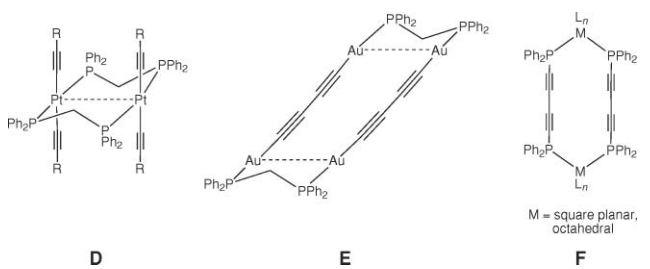

Fig. 4 Diplatinum complexes with parallel C≡C–Pt–C≡C linkages (**D**), a complex in which two butadiynediyl ligands bridge two digold endgroups (**E**), and complexes in which P–C≡C–C≡C–P linkages span two metals (**F**).

2. Structural analyses

Consider the structures of **[Pt′C$_6$Pt′]$_2$**·$4CH_2Cl_2$ (Fig. 1) and **[Pt′C$_8$Pt′]$_2$**·$0.7C_6H_{14}$·$2C_4H_8O$ (Fig. 3) first. Twisting phenomena that have no counterpart in simple diplatinum polyynediyl complexes are apparent. For starters, the two platinum coordination planes in the latter are normally coplanar. Since computational studies do not reveal any electronic driving force,[21] this presumably represents some deep-seated crystal packing preference. In

contrast, the platinum square planes at the termini of each $(C{\equiv}C)_n$ linkage in **[Pt′C$_6$Pt′]$_2$**·4CH_2Cl_2 and **[Pt′C$_8$Pt′]$_2$**·0.7C_6H_{14}·2C_4H_8O are approximately orthogonal.

We usually quantify such plane/plane angles by defining one plane consisting of the two phosphorus atoms and one platinum on one terminus, and the platinum on the opposite terminus (*e.g.*, (P_A–Pt_A–P'_A)–Pt_B or (P_1–Pt_1–P_2)–Pt_3), and a second with a reciprocal sense ((P_B–Pt_B–P'_B)–Pt_A or (P_5–Pt_3–P_6)–Pt_1). However, several other measures are obvious, such as the angle between the planes defined by platinum and the four coordinating atoms (*e.g.* ≡C_A–(P_A–Pt_A–P'_A)–C_{ipsoA} *vs.* ≡C_B–(P_B–Pt_B–P'_B)–C_{ipsoB}). Two alternatives are incorporated into Table 2, and give quite similar values.

The angle between the platinum square planes in **[Pt′C$_6$Pt′]$_2$**·4CH_2Cl_2 ranges from 78.9° to 85.5°, depending upon the measure. The values for **[Pt′C$_8$Pt′]$_2$**·0.7C_6H_{14}·2C_4H_8O range from 101.6° to 102.1°. However, the situation is altogether different for **[Pt′C$_6$Pt′]$_2$**·5CH_2Cl_2·2C_4H_8O, which as evident from Fig. 2 has nearly coplanar endgroups. The computed angle now ranges from 0.8° to 25.0°.

This dichotomy correlates to other structural features. The sp carbon chains in **[Pt′C$_6$Pt′]$_2$**·5CH_2Cl_2·2C_4H_8O, are essentially parallel, with only a slight bowing evident in the middle view of Fig. 2. However, those in **[Pt′C$_6$Pt′]$_2$**·4CH_2Cl_2 and **[Pt′C$_8$Pt′]$_2$**·0.7C_6H_{14}·2C_4H_8O are "crossed". In order to quantify this property, the carbon chains are approximated as vectors defined by the platinum atoms on opposite termini (Pt_A (Pt_1) and Pt_B (Pt_3); $Pt_{A'}$ (Pt_2) and $Pt_{B'}$ (Pt_4). Two planes are then considered, Pt_1–Pt_2–Pt_3 and Pt_2–Pt_3–Pt_4. As summarized in Table 2, these define angles of 0° for **[Pt′C$_6$Pt′]$_2$**·5CH_2Cl_2·2C_4H_8O, but 87.7° and 77.2° for **[Pt′C$_6$Pt′]$_2$**·4CH_2Cl_2 and **[Pt′C$_8$Pt′]$_2$**·0.7C_6H_{14}·2C_4H_8O.

These relationships have a number of consequences. For example, the sp carbon bridged Pt1···Pt3 distance in cross chained **[Pt′C$_6$Pt′]$_2$**·4CH_2Cl_2 is only slightly less than the non-bridged Pt1···P4 or Pt2···Pt3 distances (10.307 Å *vs.* 10.373 Å; Table 2). However, the Pt1···Pt3 distance in parallel chained **[Pt′C$_6$Pt′]$_2$**·5CH_2Cl_2·2C_4H_8O is distinctly shorter than the Pt1···Pt4 and Pt2···Pt3 distances (10.262 Å *vs.* 11.863 Å and 11.614 Å), as expected from a nearly rectangular array. In the cross chained bis(octatetraynediyl) complex **[Pt′C$_8$Pt′]$_2$**·0.7C_6H_{14}·2C_4H_8O, the bridged Pt1···Pt3 distance becomes *longer* than the non-bridged P1···P4 distance, but remains shorter than the Pt2···Pt3 distance (12.842 Å *vs.* 12.003 Å and 12.985 Å).

Interestingly, the closest carbon–carbon contacts within the crossed chained complexes are 3.61 Å and 3.27 Å, with the latter much less than the sum of the van der Waals radii (2 × 1.78 Å).[2,28] This is well within the range required for solid-state reactions of polyynes, such as topochemical polymerization.[2,29] However, the closest analogous intermolecular contacts are 10.80 Å and 9.05 Å, respectively. In contrast, the closest contact between the nearly parallel sp carbon chains in [**Pt′C$_6$Pt′**]$_2$·5CH_2Cl_2·2C_4H_8O is 4.96 Å, which is much greater than the sum of the van der Waals radii. Accordingly, the crystal density, which is sometimes used to gauge the relative stabilities of polymorphs,[20] is lower (1.587 *vs.* 1.711 Mg m^{-3}).

The bond lengths and angles associated with the $Pt(C{\equiv}C)_3Pt$ and $Pt(C{\equiv}C)_4Pt$ segments in these complexes are similar and close to those of **PtC$_6$Pt**, **PtC$_8$Pt**, and related compounds.[10,15,21] The 1,3-diphosphine ligands adopt comparable backbone conformations in all structures. As shown in Table 2, nine of the twelve P–C–C–C torsion angles are within 12° of that for an idealized *anti* conformation (180°).

In **PtC$_6$Pt**, **PtC$_8$Pt**, and related compounds, stacking interactions involving the platinum-bound pentafluorophenyl ligands and phosphorus-bound aryl groups are usually found.[10-12,15,30] The physical basis of this phenomenon, which has abundant precedent with organic molecules and mixed crystals, is well understood.[31] Some $C_6H_5/C_6F_5/C_6H_5$ interactions are apparent in Fig. 1–3, as evidenced by the shorter centroid–centroid distances in Table 2 (3.597–3.882 Å). However, some rings show much greater spacings (3.975–4.796 Å). Accordingly, the *average* centroid–centroid spacings—3.85, 4.00, and 4.00 Å, respectively—are greater than those in model complexes such as **PtC$_6$Pt** (3.66 Å) and **PtC$_8$Pt** (3.67 Å).

3. Future challenges

The conformational diversity reflected in the crystal structures of **[Pt′C$_x$Pt′]$_2$** indicate that such complexes should have a range of accessible conformations in solution. Nonetheless, it has so far proved difficult to realize well-defined transannular reactions. This is somewhat surprising in view of the well defined cycloadditions that have been realized at moderate temperatures with species of the type **F** in Fig. 4.[27b,c] However, **[Pt′C$_x$Pt′]$_2$** are robust solids that begin to decompose only at 186–269 °C, and are much more thermally stable than **F** in solution.

Intuitively, species that can function as multistranded molecular wires would seem to offer distinct advantages in molecular electronics. However, to our knowledge the literature on this subject is scant, and limited to theoretical studies and current/voltage dependencies of junction spanning monolayers.[32] In this context, it may be possible to fine tune chain–chain spacings by employing 1,4-diphosphines, or conformationally restricted 1,3-diphosphines such as those based upon *meta*-disubstituted arenes. Single molecule break junction measurements involving somewhat related platinum alkynyl complexes have established insulator properties.[33] However, even if the title molecules behaved similarly, they would still fulfil other criteria for molecular wires.[5]

There are also reasonable chances that this chemistry can be extended to triply stranded systems. An attractive 1,3,5-triphosphine, $Ph_2P(CH_2)_3PPh(CH_2)_3PPh_2$, is readily available,[34] and routes to doubly protected derivatives such as $Ph_2P(X)(CH_2)_3PPh(CH_2)_3P(X)Ph_2$, which could be used to template the first $Pt(C{\equiv}C)_nPt$ strand, are easily envisioned. Indeed, polyphosphines template a variety of fascinating reactions. For example, when two equivalents of the tetraphosphine *meso*-$Ph_2PCH_2PPhCH_2PPhCH_2PPh_2$ are treated with four equivalents of $AuClPPh_3$, a tetragold complex can be isolated with four *trans*-P–Au–P linkages.[35]

In conclusion, we have established that the 1,3-diphosphine $Ph_2P(CH_2)_3PPh_2$ is capable of assembling $Pt(C{\equiv}C)_nPt$ and presumably other $M(C{\equiv}C)_nM$ units into tetrametallic "bundles", with the phosphorus atoms spanning metals that terminate separate polyynediyl moieties. The sp carbon chains can adopt parallel or "crossed" conformations. These architecturally novel species complement other assemblies based upon $M(C{\equiv}C)_nM$ units, such as polygons and extended $L_yM[(C{\equiv}C)_nML_y]_z(C{\equiv}C)_nML_y$ arrays. Finally, a detailed model for the reactivity of

diplatinum polyynediyl complexes with various α,ω-diphosphines $Ar_2P(CH_2)_mPAr_2$ has been developed, further tests and extensions of which will be reported in due course.

Experimental section

General

Reactions were conducted under N_2 atmospheres. Workups were carried out in air unless noted. Chemicals were treated as follows: hexane and THF, distilled from Na/benzophenone; methanol and CH_2Cl_2, freshly distilled; $Ph_2P(CH_2)_3PPh_2$ (dppp, Lancaster), $Ph_2P(CH_2)_2PPh_2$ (dppe, TCI), PEt_3 (Aldrich, 1.0 M in THF), and NMR solvents, used as received. NMR spectra were recorded at ambient probe temperatures on standard 400 MHz spectrometers unless another field strength is noted, and referenced as follows: ^1H, ^{13}C, residual solvent signals; ^{31}P, internal H_3PO_4 capillary ($\delta = 0.00$ ppm); ^{19}F, external C_6F_6 ($\delta = -164.9$ ppm). IR and UV-visible spectra were recorded on ASI ReactIR-1000 and Shimadzu model 3102 spectrometers. Mass spectra were recorded on a Micromass Zabspec instrument. Microanalyses were conducted on a Carlo Erba EA 1110 instrument. DSC and TGA data were recorded with a Mettler-Toledo DSC-821 instrument.[36]

trans,*trans*,*trans*,*trans*-$(C_6F_5)Pt(C{\equiv}C)_3Pt(C_6F_5)(PPh_2(CH_2)_3Ph_2P)_2(C_6F_5)Pt(C{\equiv}C)_3Pt(C_6F_5)(PPh_2(CH_2)_3Ph_2P)_2$ ([Pt′C_6Pt′]$_2$)

A Schlenk flask was charged with *trans*,*trans*-$(C_6F_5)(p\text{-}tol_3P)_2Pt(C{\equiv}C)_3Pt(P\textit{p}\text{-}tol_3)_2(C_6F_5)$ (**PtC_6Pt**; 0.396 g, 0.197 mmol)[15] and THF (50 mL). The mixture was stirred until all **PtC_6Pt** had dissolved. Then solid $Ph_2P(CH_2)_3PPh_2$ (0.203 g, 0.493 mmol) was added in one portion. After 12 h, the sample was concentrated to *ca.* 5 mL, and hexane (25 mL) was added. The mixture was further concentrated to *ca.* 10 mL. The solid was collected by filtration, washed with hexane (2 × 10 mL), and dried by oil pump vacuum to give **[Pt′C_6Pt′]$_2$** as a yellow powder (0.305 g, 0.094 mmol, 95%), dec pt 220 °C (capillary, gradual darkening without melting). DSC: endotherm with T_i 117.4 °C, T_e 169.1 °C, T_c 203.1 °C, T_f 204.0 °C; exotherm with T_i 190.7 °C, T_e 195.9 °C, T_c 229.1 °C, T_i 230.1 °C; TGA: first mass loss regime, T_i 268.6 °C, T_e 275.5 °C, T_f 323.1 °C; second mass loss regime, T_i 330.3 °C, T_f 504.3 °C; Calcd for $C_{144}H_{104}F_{20}P_8Pt_4$: C, 53.34; H, 3.23. Found C, 53.91; H, 3.76.

NMR (δ, CD_2Cl_2), ^1H 7.98 (m, 4H, Ph), 7.51 (m, 6H, Ph), 7.20 (m, 2H, Ph), 6.93 (m, 8H, Ph), 3.62 (m, 1H, CH_2), 3.12 (m, 2H, CH_2), 2.70 (m, 3H, CH_2); $^{13}C\{^1H\}$[37] 146.3 (dm, $^3J_{CF} = 222$ Hz, *o* to Pt), 136.9 (overlapping m, *m*/*p* to Pt), 135.0 (br s,[37a] *o* to P), 131.5 (br s,[37a] *o* to P), 131.4 (s, *p* to P), 129.9 (s, *p* to P), 128.9 (br s,[37a] *m* to P), 127.8 (br s,[37a] *m* to P), 94.4 (br s, Pt*C*≡C),[38] 94.1 (s, PtC≡*C*), 61.1 (s, PtC≡C*C*), 30.8 (m, PCH_2), 24.4 (m, PCH_2CH_2); $^{31}P\{^1H\}$ 13.0 (s, $^1J_{PPt} = 2611$ Hz).[16]

IR (cm^{-1}, powder film), 2107 (br w, $\nu_{C\equiv C}$). UV-vis (nm, 1.25×10^{-5} M in CH_2Cl_2 (ε, M^{-1} cm^{-1}), 307 (60000), 342 (25600), 367 (14500). MS (*m*/*z*, positive FAB, 3-NBA),[39] 3241 (M^+, 15%), 774 ($dpppPtC_6F_5^+$, 15%), 606 ($dpppPt^+$, 100%).

[Pt′C_8Pt′]$_2$

A Schlenk flask was charged with **PtC_8Pt** (0.200 g, 0.098 mmol)[15] and THF (40 mL). Solid $Ph_2P(CH_2)_3PPh_2$ (0.097 g, 0.235 mmol) was then added in one portion to the solution. After 16 h, the mixture was concentrated to *ca.* 5 mL, and hexane (30 mL) was added. The solid was collected by filtration, washed with hexane (2 × 10 mL), and dried by oil pump vacuum to give **[Pt′C_8Pt′]$_2$** as a yellow powder (0.131 g, 0.039 mmol, 81%), dec pt 186 °C (capillary, gradual darkening without melting). DSC: exotherm with T_i 200.8 °C, T_e 245.1 °C, T_f 269.9 °C; TGA: T_i 265.8 °C, T_e 305.0 °C, T_f 504.4 °C. Calcd for $C_{148}H_{104}F_{20}P_8Pt_4$: C, 54.02; H, 3.19. Found C, 54.01; H, 3.33.

NMR (δ, $CDCl_3$), ^1H 7.96 (m, 4H, *o* to P), 7.51 (m, 4H, *o* to P and 2H, *p* to P), 7.16 (m, 2H, *p* to P), 7.01 (m, 8H, *m* to P), 3.76 (m, 1H, CH_2), 3.15 (m, 2H, CH_2), 2.73 (m, 1H, CH_2), 2.64 (m, 2H, CH_2); $^{13}C\{^1H\}$[37] 146 (v br m, *o* to Pt), 137 (v br overlapping m, *m*/*p* to Pt), 135.1 (br s,[37a] *o* to P), 131.6 (s, *p* to P), 131.5 (br s,[37a] *o* to P), 130.0 (s, *p* to P), 129.0 (br s,[37a] *m* to P), 127.9 (br s,[37a] *m* to P), 93.8 (s, PtC≡*C*), 64.7 (s, PtC≡C*C*), 58.7 (s, PtC≡CC≡*C*), 31.2 (m, PCH_2), 24.1 (m, PCH_2CH_2); $^{31}P\{^1H\}$ 13.5 (s, $^1J_{PPt} = 2606$ Hz).[16]

IR (cm^{-1}, powder film), 2150 (m, $\nu_{C\equiv C}$), 2007 (w, $\nu_{C\equiv C}$). UV-vis (nm, 1.25×10^{-5} M in CH_2Cl_2 (ε, M^{-1} cm^{-1}), 310 (129000), 322 (193000), 352 (12600), 379 (9800), 410 (6000). MS (*m*/*z*, positive FAB, 3-NBA):[39] 3291 (M^+, 10%), 774 ($dpppPtC_6F_5^+$, 10%), 606 ($dpppPt^+$, 100%).

[Pt′C_4Pt′]$_2$

A Schlenk flask was charged with **PtC_4Pt** (0.100 g, 0.050 mmol)[15] and THF (100 mL). The sample was stirred until all **PtC_4Pt** had dissolved. Then solid $Ph_2P(CH_2)_3PPh_2$ (0.052 g, 0.126 mmol) was added in one portion. After 16 h, the mixture was concentrated to *ca.* 10 mL, and hexane (25 mL) was added. The solid was collected by filtration, washed with hexane (2 × 10 mL), and dried by oil pump vacuum to give **[Pt′C_4Pt′]$_2$** as a white powder (0.062 g, 0.019 mmol, 39%), dec pt 269 °C (capillary, slight darkening) to 275 °C (black liquid). Calcd for $C_{140}H_{104}F_{20}P_8Pt_4$: C, 52.64; H, 3.28. Found C, 52.45; H, 3.28.

NMR (δ, C_6D_5Br), ^1H, 8.13 (br m, 4H, Ph), 7.28 (br m, 16H, Ph), 3.97 (br m, 1H, CH_2), 2.57 (br m, 5H, CH_2); $^{31}P\{^1H\}$ 14.8 (s, $^1J_{PPt} = 2658$ Hz).[16] MS (*m*/*z*, positive FAB, 3-NBA),[39] 3192 (M^+, 45%), 3114 (M–Ph^+, 10%), 774 ($dpppPtC_6F_5^+$, 28%), 606 ($dpppPt^+$, 100%).

[Pt′C_{12}Pt′]$_2$

An analogous reaction was conducted with **PtC_{12}Pt**.[15] This gave an orange powder with some properties appropriate for **[Pt′C_{12}Pt′]$_2$**, but which did not dissolve in CH_2Cl_2 and was only very slightly soluble in THF. NMR (δ, THF-d_8), $^{31}P\{^1H\}$ 13.3 (s, $^1J_{PPt} = 2565$ Hz).[16] DSC: endotherm with T_i 107.1 °C, T_e 140.5 °C, T_c 172.7 °C, T_f 178.1 °C; exotherm with T_e 213.5 °C; TGA: T_i 239.8 °C, T_e 258.0 °C, T_f 402.9 °C. Calcd for $C_{156}H_{104}F_{20}P_8Pt_4$: C, 55.33; H, 3.10. Found C, 55.33; H, 3.27.

Reaction of [Pt′C_4Pt′]$_2$ and PEt_3

A Schlenk flask was charged with **[Pt′C_4Pt′]$_2$** (0.1576 g, 0.04934 mmol) and THF (20 mL). Then PEt_3 (0.50 mL, 0.50 mmol, 1.0M in THF) was added to the white suspension with stirring. After 18 h, an aliquot of the suspension was removed and a $^{31}P\{^1H\}$ NMR spectrum recorded. Data (δ, THF, 202 MHz):

15.3 (s, **[Pt′C$_4$Pt′]$_2$**), 13.3 (s, $^1J_{PPt}$ = 2450 Hz,[16] *trans*,*trans*-(C$_6$F$_5$)(Et$_3$P)$_2$Pt(C≡C)$_2$Pt(PEt$_3$)$_2$(C$_6$F$_5$)),[17] –16.8 (s, dppp),[40] –18.5 (s, PEt$_3$).[41] Area ratio of the 15.3 and 13.3 ppm signals: 6 : 94.

***cis*,*cis*-(P̄Ph$_2$(CH$_2$)$_2$Ph$_2$P)(C$_6$F$_5$)Pt-(C≡C)$_4$Ṕt(C$_6$F$_5$)(PPh$_2$(CH$_2$)$_2$Ph$_2$P̄) (Pt″C$_8$Pt″)**

A Schlenk flask was charged with **PtC$_8$Pt** (0.124 g, 0.0610 mmol) and THF (20 mL). Solid dppe (0.052 g, 0.131 mmol) was added with stirring. After 16 h, the precipitate was isolated by filtration, washed with Et$_2$O (3 × 10 mL), and dried by oil pump vacuum to give **Pt″C$_8$Pt″** as a light yellow solid (0.072 g, 0.045 mmol, 73%), dec pt 245 °C (capillary, slight darkening) to 280 °C (black solid; no further change to 300 °C). Calcd for C$_{72}$H$_{48}$F$_{10}$P$_4$Pt$_4$: C, 53.47; H, 2.99. Found: C, 53.19; H, 2.86.

NMR (δ, DMF-d_7), ^{1}H (500 MHz) 8.06–8.01 (m, 8H, Ph), 7.62–7.52 (m, 24H, Ph), 7.47–7.44 (m, 8H, Ph), 2.88–2.78 (m, 4H, CH$_2$), 2.67–2.57 (m, 4H, CH$_2$); ^{13}C{^{1}H} (125 MHz) 147.2 (m, *o* to Pt),[42] 138.8, 136.9 (2 m, *m*/*p* to Pt),[42] 134.5 (d, $^2J_{CP}$ = 11.1 Hz, *o* to P), 134.2 (d, $^2J_{CP}$ = 11.1 Hz, *o* to P′), 132.8–132.7 (2 overlapping d, $^4J_{CP}$ = 2.8 or 3.4 Hz, *p* to P/P′), 131.3 (d, $^1J_{CP}$ = 54.1 Hz, *i* to P), 130.2 (d, $^1J_{CP}$ = 55.0 Hz, *i* to P′), 130.1 (d, $^3J_{CP}$ = 10.8 Hz, *m* to P),[37b] 129.8 (d, $^3J_{CP}$ = 10.7 Hz, *m* to P′),[37b] 105.1 (m, PtC≡C),[42] 95.8 (m, PtC≡*C*),[42] 64.7 (s, PtC≡C*C*), 60.0 (s, PtC≡CC≡*C*), 28.9–28.5, 26.9–26.5 (2 m, CH$_2$);[42] ^{31}P{^{1}H} (202 MHz) 44.7 (d, $^2J_{PP}$ = 6.2 Hz, $^1J_{PPt}$ = 2358 Hz,[16] *trans* to C≡C), 41.8–41.6 (m, $^1J_{PPt}$ = 2255 Hz,[16] *trans* to C$_6$F$_5$); ^{19}F (470 MHz) –112.82 to –112.94 (m, $^3J_{FPt}$ = 314 Hz, 4F, *o* to Pt), –159.34 (t, $^3J_{FF}$ = 19.7.0 Hz, 2F, *p* to Pt), –160.80 to –160.91 (m, 4F, *m* to Pt).

IR (cm^{-1}, powder film), 3055 (w), 2862 (w), 2149 (m, $\nu_{C\equiv C}$), 2006 (w, $\nu_{C\equiv C}$). MS (*m*/*z*, positive FAB), 1616 (M$^+$, 43%), 1024 (dppePt(C$_6$F$_5$)(C≡C)$_4^+$, 19%), 760 (dppePtC$_6$F$_5^+$, 50%), 593 (dppePt$^+$, 100%).

Pyrolyses

A solid sample of **[Pt′C$_8$Pt′]$_2$** was kept at 200 °C for 1 h. An IR spectrum showed a new band at 2077 cm^{-1}, together with those of the starting material. The sample was kept at 250 °C for 1 h. An IR spectrum showed only the band at 2077 cm^{-1}.

Cyclic voltammetry

A BAS CV-50W Voltammetric Analyzer (Cell Stand C3) with the program CV-50W (version 2.0) was employed. Cells were fitted with platinum working and counter electrodes, and a silver wire pseudoreference electrode. All CH$_2$Cl$_2$ solutions were 7–9 × 10^{-4} M in complex, 0.1 M in *n*-Bu$_4$N$^+$ BF$_4^-$ (crystallized from ethanol–hexane and dried by oil pump vacuum), and prepared under nitrogen. Ferrocene was subsequently added, and calibration voltammograms recorded (ambient laboratory temperature, 22.5 ± 1 °C). Data: see Table 3.

Crystallography

A. A CH$_2$Cl$_2$ solution of **[Pt′C$_6$Pt′]$_2$** was layered with methanol (room temperature). After six d, a yellow prism was selected. Data were collected as outlined in Table 1. Cell parameters were obtained from 10 frames using a 10° scan and refined with 15811 reflections. Lorentz, polarization, and absorption corrections[43] were applied. The space group was determined from systematic absences and subsequent least-squares refinement. The structure was solved by direct methods on F^2. The parameters were refined with all data by full-matrix-least-squares on F^2 using SHELXL-97.[44] All non-hydrogen atoms except for C200 and C201 were refined with anisotropic thermal parameters. The hydrogen atoms were fixed in idealized positions using a riding model. Scattering factors were taken from literature.[45] The unit cell contained sixteen CH$_2$Cl$_2$ molecules. Half were disordered and refined to a 68 : 32 occupancy ratio (C200/Cl21/Cl22; C201/Cl2a/Cl2b). The complex exhibited a C$_2$ axis defined by the midpoints of the platinum–platinum vector on each terminus.

B. The THF solvent was removed from a reaction mixture containing **[Pt′C$_6$Pt′]$_2$**. The residue was dissolved in CH$_2$Cl$_2$ and layered with methanol (room temperature). After four d, a yellow prism was analyzed as in procedure A. The structure was solved and refined in an identical manner (using 18238 reflections). The unit cell contained ten CH$_2$Cl$_2$ and four THF molecules. One CH$_2$Cl$_2$ molecule (C500/C501/Cl51) seemed to be disordered over two positions, but the data were too weak to resolve this. Hence, the occupancy was set to 50% and the atoms refined isotropically. The complex exhibited an inversion center at the middle of the rectangle defined by the four platinum atoms.

C. A THF solution of **[Pt′C$_8$Pt′]$_2$** was layered with hexane (room temperature). After 5 d, a pale yellow needle was selected and data were collected as outlined in Table 1. The integrated intensity information for each reflection was obtained by reduction of the data frames with the program APEX2.[46] Cell parameters were obtained from 60 frames using three sets of ω scans, and final values were obtained by the least squares refinement of 119008 reflections.[46] Lorentz and polarization corrections were applied. Data were scaled, and absorption corrections[44] were applied. The structure was solved by direct methods using SHELXS-97[44] and refined (weighted least squares refinement on F^2) using SHELXL-97.[44,47] The hydrogen atoms were placed in idealized positions, and refined using a riding model. The unit cell contained THF (8 molecules) and C$_6$H$_{14}$ (partial site occupancy; refined to 2.8). Non-hydrogen atoms were refined with anisotropic thermal parameters. Some carbon and fluorine atoms of the pentafluorophenyl groups exhibited elongated thermal ellipsoids, but no attempt was made to model this possible wagging disorder. The complex contained a C$_2$ axis defined by the midpoints of the platinum–platinum vectors involving opposite termini and sp chains.

Acknowledgements

We thank the US National Science Foundation (CHE-0719267), the Deutsche Forschungsgemeinschaft (DFG, SFB 583), the Humboldt Foundation (Fellowship to G. R. O.), and Johnson Matthey PMC (platinum loans) for support.

References

1 M. I. Bruce and P. J. Low, *Adv. Organomet. Chem.*, 2004, **50**, 179.
2 S. Szafert and J. A. Gladysz, *Chem. Rev.*, 2003, **103**, 4175; S. Szafert and J. A. Gladysz, *Chem. Rev.*, 2006, **106**, PR1–PR33.
3 F. Paul, C. Lapinte, in *Unusual Structures and Physical Properties in Organometallic Chemistry*, M. Gielen, R. Willem, B. Wrackmeyer, ed.; Wiley: New York, 2002, pp. 220–291.

4 (*a*) M. I. Bruce, P. J. Low, K. Costuas, J.-F. Halet, S. P. Best and G. A. Heath, *J. Am. Chem. Soc.*, 2000, **122**, 1949; (*b*) H. Jiao, K. Costuas, J. A. Gladysz, J.-F. Halet, M. Guillemot, L. Toupet, F. Paul and C. Lapinte, *J. Am. Chem. Soc.*, 2003, **125**, 9511.

5 (*a*) As defined by Lehn, molecular wires encompass three distinct modes of electron flow: electron transport, electron hopping, and electron conduction: J.-M. Lehn, *Supramolecular Chemistry*, VCH: Weinheim, 1995, Chapter 8.3.2; (*b*) See also P. J. Low, *Dalton Trans.*, 2005, 2821.

6 (*a*) S. Takahashi, M. Kariya, T. Yatake, K. Sonogashira and N. Hagihara, *Macromolecules*, 1978, **11**, 1063; (*b*) K. Sonogashira, S. Kataoka, S. Takahashi and N. Hagihara, *J. Organomet. Chem.*, 1978, **160**, 319; (*c*) K. Sonogashira, K. Ohga, S. Takahashi and N. Hagihara, *J. Organomet. Chem.*, 1980, **188**, 237; (*d*) R. D. Markwell, I. S. Butler, A. K. Kakkar, M. S. Khan, Z. H. Al-Zakwani and J. Lewis, *Organometallics*, 1996, **15**, 2331.

7 Q. Zheng, F. Hampel and J. A. Gladysz, *Organometallics*, 2004, **23**, 5896.

8 (*a*) S. M. ALQaisi, K. J. Galat, M. Chai, D. G. Ray, III, P. L. Rinaldi, C. A. Tessier and W. J. Youngs, *J. Am. Chem. Soc.*, 1998, **120**, 12149; (*b*) M. I. Bruce, K. Costuas, J.-F. Halet, B. C. Hall, P. J. Low, B. K. Nicholson, B. W. Skelton and A. H. White, *J. Chem. Soc., Dalton Trans.*, 2002, 383; (*c*) M. Janka, G. K. Anderson and N. P. Rath, *Organometallics*, 2004, **23**, 4382.

9 For a tetraplatinum square with $(C{\equiv}C)_2Au(C{\equiv}C)_2$ edges, see M. I. Bruce, B. C. Hall, B. W. Skelton, M. E. Smith and A. H. White, *J. Chem. Soc., Dalton Trans.*, 2002, 995.

10 G. R. Owen, J. Stahl, F. Hampel and J. A. Gladysz, *Chem.–Eur. J.*, 2008, **14**, 73.

11 J. Stahl, W. Mohr, L. de Quadras, T. B. Peters, J. C. Bohling, J. M. Martín-Alvarez, G. R. Owen, F. Hampel and J. A. Gladysz, *J. Am. Chem. Soc.*, 2007, **129**, 8282.

12 (*a*) L. de Quadras, E. B. Bauer, W. Mohr, J. C. Bohling, T. B. Peters, J. M. Martín-Alvarez, F. Hampel and J. A. Gladysz, *J. Am. Chem. Soc.*, 2007, **129**, 8296; (*b*) L. de Quadras, E. B. Bauer, J. Stahl, F. Zhuravlev, F. Hampel and J. A. Gladysz, *New J. Chem.*, 2007, **31**, 1594.

13 (*a*) M. Sato, E. Mogi and S. Kumakura, *Organometallics*, 1995, **14**, 3157; (*b*) A. L. Sadowy, M. J. Ferguson, R. McDonald and R. R. Tykwinski, *Organometallics*, 2008, **27**, 6321.

14 G. R. Owen, F. Hampel and J. A. Gladysz, *Organometallics*, 2004, **23**, 5893.

15 W. Mohr, J. Stahl, F. Hampel and J. A. Gladysz, *Chem.–Eur. J.*, 2003, **9**, 3324.

16 This coupling represents a satellite (d, ^{195}Pt = 33.8%), and is not reflected in the peak multiplicity given.

17 J. Stahl, J. C. Bohling, T. B. Peters, L. de Quadras and J. A. Gladysz, *Pure Appl. Chem.*, 2008, **80**, 459.

18 Q. Zheng, J. C. Bohling, T. B. Peters, A. C. Frisch, F. Hampel and J. A. Gladysz, *Chem.–Eur. J.*, 2006, **12**, 6486.

19 S. O. Grim, R. L. Keiter and W. McFarlane, *Inorg. Chem.*, 1967, **6**, 1133.

20 T. L. Threlfall, *Analyst*, 1995, **120**, 2435.

21 F. Zhuravlev and J. A. Gladysz, *Chem.–Eur. J.*, 2004, **10**, 6510.

22 (*a*) M. Brady, W. Weng, Y. Zhou, J. W. Seyler, A. J. Amoroso, A. M. Arif, M. Böhme, G. Frenking and J. A. Gladysz, *J. Am. Chem. Soc.*, 1997, **119**, 775; (*b*) R. Dembinski, T. Bartik, B. Bartik, M. Jaeger and J. A. Gladysz, *J. Am. Chem. Soc.*, 2000, **122**, 810; (*c*) W. E. Meyer, A. J. Amoroso, C. R. Horn, M. Jaeger and J. A. Gladysz, *Organometallics*, 2001, **20**, 1115; (*d*) C. R. Horn and J. A. Gladysz, *Eur. J. Inorg. Chem.*, 2003, 2211.

23 (*a*) K. Rana, B. Kaur, B. Kumar, H. Kumar and R. D. Anand, *Indian J. Chem.*, 2001, **40B**, 1170; (*b*) A. V. Vasil'ev and A. P. Rudenko, *Russian J. Org. Chem.*, 1997, **33**, 1555 (*Zh. Org. Khim.* **1997**, *33*, 1639).

24 L. de Quadras, J. Stahl, F. Zhuravlev and J. A. Gladysz, *J. Organomet. Chem.*, 2007, **692**, 1859.

25 N. W. Alcock, T. J. Kemp, P. G. Pringle, P. Bergamini and O. Traverso, *J. Chem. Soc., Dalton Trans.*, 1987, 1659, and references therein.

26 (*a*) H.-B. Xu, L.-X. Shi, E. Ma, L.-Y. Zhang, Q.-H. Weis and Z.-N. Chen, *Chem. Commun.*, 2006, 1601; (*b*) H.-B. Xu, L.-Y. Zhang, Z.-L. Xie, E. Ma and Z.-N. Chen, *Chem. Commun.*, 2007, 2744.

27 (*a*) D. Xu and B. Hong, *Angew. Chem., Int. Ed.*, 2000, **39**, 1826; D. Xu and B. Hong, *Angew. Chem.*, 2000, **112**, 1896; (*b*) M. P. Martin-Redondo, L. Scoles, B. T. Sterenberg, K. A. Udachin and A. J. Carty, *J. Am. Chem. Soc.*, 2005, **127**, 5038; (*c*) J. A. Tsui and B. T. Sterenberg, *Organometallics*, 2009, **28**, 4906.

28 A. Bondi, *J. Phys. Chem.*, 1964, **68**, 441.

29 (*a*) V. Enkelmann, *Adv. Polym. Sci.*, 1984, **63**, 91; (*b*) J. Xiao, M. Yang, J. W. Lauher and F. W. Folwer, *Angew. Chem., Int. Ed.*, 2000, **39**, 2132; J. Xiao, M. Yang, J. W. Lauher and F. W. Fowler, *Angew. Chem.*, 2000, **112**, 2216.

30 H. Kuhn, F. Hampel and J. A. Gladysz, *Organometallics*, 2009, **28**, 4979.

31 K. Reichenbächer, H. I. Süss and J. Hullinger, *Chem. Soc. Rev.*, 2005, **34**, 22.

32 (*a*) S. N. Yaliraki and M. A. Ratner, *J. Chem. Phys.*, 1998, **109**, 5036; (*b*) M. Magoga and D. Joachim, *Phys. Rev. B: Condens. Matter Mater. Phys.*, 1999, **59**, 16011; (*c*) N. D. Lang and P. Avouris, *Phys. Rev. B: Condens. Matter Mater. Phys.*, 2000, **62**, 7325; (*d*) J. G. Kushmerick, J. Naciri, J. C. Yang and R. Shashidhar, *Nano Lett.*, 2003, **3**, 897.

33 (*a*) M. Mayor, C. von Hänisch, H. B. Weber, J. Reichert and D. Beckmann, *Angew. Chem., Int. Ed.*, 2002, **41**, 1183; M. Mayor, C. von Hänisch, H. B. Weber, J. Reichert and D. Beckmann, *Angew. Chem.*, 2002, **114**, 1228; (*b*) See also S. Ballmann, W. Hieringer, D. Secker, Q. Zheng, J. A. Gladysz, A. Görling and H. B. Weber, *ChemPhysChem*, 2010, **11**, DOI: 10.1002/cphc.200900974.

34 (*a*) D. L. Dubois, W. H. Myers and D. W. Meek, *J. Chem. Soc., Dalton Trans.*, 1975, 1011; (*b*) R. D. Waid and D. W. Meek, *Inorg. Chem.*, 1984, **23**, 778; (*c*) R. B. King and J. C. Cloyd Jr., *Inorg. Chem.*, 1975, **14**, 1550.

35 Y. Takemura, H. Takenaka, T. Nakajima and T. Tanase, *Angew. Chem., Int. Ed.*, 2009, **48**, 2157; Y. Takemura, H. Takenaka, T. Nakajima and T. Tanase, *Angew. Chem.*, 2009, **121**, 2191.

36 H. K. Cammenga and M. Epple, *Angew. Chem., Int. Ed. Engl.*, 1995, **34**, 1171; H. K. Cammenga and M. Epple, *Angew. Chem.*, 1995, **107**, 1284.

37 (*a*) The P*Ph* groups are diastereotopic, leading to two sets of ^{13}C NMR signals for which the expected couplings (J_{CP}) were often not resolved. The *ipso* PPh ^{13}C signal of **[Pt′C$_6$Pt′]$_2$**, and the *ipso* PPh, PtC$_6$F$_5$, and Pt*C*≡C ^{13}C signals of **[Pt′C$_8$Pt′]$_2$**, were not observed; (*b*) The ^{13}C NMR signal with the chemical shift closest to benzene can be assigned to the *meta* carbon atom of the phenyl ring: B. E. Mann, *J. Chem. Soc., Perkin Trans. 2*, 1972, 30. With **Pt″C$_8$Pt″**, the designations P/P′ are arbitrary.

38 Phosphorus coupling would be expected based upon spectra of related compounds; however, the signal/noise ratio was not sufficient.

39 The mass spectrum also showed a peak corresponding to the molecular ion plus O_2H. Analogous ions are not observed for diplatinum complexes such as **PtC$_6$Pt** or **PtC$_8$Pt**.

40 S. U. Son, Y. Jang, K. Y. Yoon, E. Kang and T. Hyeon, *Nano Lett.*, 2004, **4**, 1147.

41 J. Tong, S. Liu, S. Zhang and S. Z. Li, *Spectrochim. Acta Part A*, 2007, **A67**, 837.

42 This signal was barely detectable (poor signal/noise ratio), but was verified by a separate ^{13}C{^{1}H,^{19}F,^{31}P} NMR spectrum.

43 (*a*) *"Collect" data collection software*, Nonius B.V., 1998; (*b*) "Scalepack" data processing software: Z. Otwinowski, W. Minor, in *Methods in Enzymology* 1997, 276 (Macromolecular Crystallography, Part A), 307.

44 G. M. Sheldrick, *Acta Crystallogr., Sect. A: Crystallogr.*, 2008, **A64**, 112.

45 D. T. Cromer, J. T. Waber, in *International Tables for X-ray Crystallography*, J. A. Ibers, W. C. Hamilton, ed.; Kynoch: Birmingham, England, 1974.

46 Bruker (2007) *APEX2*. Bruker AXS Inc., 5465 East Cheryl Parkway, Madison, WI 53711-5373 USA.

47 L. J. Barbour, *J. Supramol. Chem.*, 2001, **1**, 189.